Role of pulling direction in understanding the energy landscape of proteins

R. Rajesh

Institute of Mathematical Sciences, CIT Campus, Taramani, Chennai-600113, India

D. Giri

Department of Applied Physics, IT, Banaras Hindu University, Varanasi 221 005, India

I. Jensen

Department of Mathematics and Statistics, The University of Melbourne, Victoria 3010, Australia

S. Kumar

Department of Physics, Banaras Hindu University, Varanasi 221 005, India

Single-molecule force spectroscopy provide details of the underlying energy surfaces of proteins which are essential to the understanding of their unfolding process. Recently, it has been observed experimentally that by pulling proteins in different directions relative to their secondary structure, one can gain a better understanding of the shape of the energy landscape. We consider simple lattice models which are anisotropic in nature to study the response of a force in unfolding of a polymer. Our analytical solution of the model, supported by extensive numerical calculations, reveal that the force temperature diagrams are very different depending on the direction of the applied force. We find that either unzipping or shearing kind transitions dominate the dynamics of the unfolding process depending solely on the direction of the applied force.

I. INTRODUCTION

Recent experiments have shown that the energy landscapes governing the mechanical unfolding of proteins are different from the energy landscapes governing the thermal or chemical unfolding [1–5]. Until recently it was believed that all residues of any given protein contribute equally to the thermodynamic stability of globular proteins, with the stability of the protein structure being provided by its hydrophobic core [6,7]. It was therefore expected that the mechanical unfolding of a protein should be insensitive to the direction of the applied force. Surprisingly, recent experiments have shown that a protein's resistance to unfolding depends strongly on the pulling direction [8–11]. Varying the pulling direction also gives Angstrom precise information about the structure of biomolecules [12,13].

Force extension curves obtained by single molecule experiments (unfolding of proteins, stretching of DNA) are often described by the wormlike chain (WLC) model or freely jointed chain (FJC) model [14,15]. The mechanical properties of the FJC and WLC models are well understood, and the usefulness of these models stems from their simplicity, which means that the analytic expression for the extension can be written in a very simple form [16,17]. The only parameter appearing in the description of these models is the persistence length of the polymer chain. The force-extension curves obtained from these models [16–18] show an excellent agreement with the main features observed in early experiments [1–4]. Since the FJC and WLC models are isotropic, in order to study the resistance of a protein to unfolding when the pulling geometry is changed, one would have to use different persistence lengths (along different directions) to fit the force extension curves [8,9,17]. So when a polymer has been pulled along the x direction one may use a certain

persistence length which reproduces the observed force-extension curve. If the pulling direction is changed another persistence length is used to fit the new force-extension curve. However, the underlying model is still isotropic and the procedure is somewhat *ad hoc* and does not provide a unified approach to the modeling of the anisotropic behavior [19,20] seen in experiments. Equally importantly these simple models do not incorporate excluded volume effects in its description.

In a recent paper Kumar and Giri [21] used partially directed self-avoiding walks (PDSAWs) to model anisotropic biomolecules. When a force is applied to one end of the chain it undergoes a transition from a folded to an unfolded state. Numerical studies based on a chain size of $N=30$ showed that when the chain is being pulled along the preferred direction of the polymer, the nature of the transition is akin to unzipping, but when force is applied perpendicular to the preferred direction, the transition is akin to shearing.

In Sec. II we provide the analytical solution of the model and show that a change in the pulling direction gives rise to different phase diagrams even in the thermodynamic (infinite chain length) limit. In Sec. III we report on an algorithmic breakthrough which has enabled us to increase the chain length to $N=150$ which is five times longer than in the previous study [21]. The longer series are used to obtain numerical estimates for the phase boundary in excellent agreement with the exact results. In this section we also discuss the relevance of two ensembles namely, the constant force ensemble (CFE) and the constant distance ensemble (CDE) which are appropriate when describing different experimental setups. With the enhanced information about the exact density of states of longer chains, we are able to study precisely finite-size effects which are crucial to all single molecule experiments. In particular we find marked differences
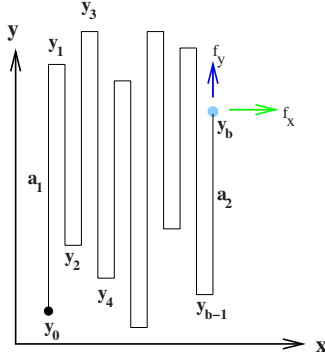
FIG. 1. (Color online) Schematic representation of a PDSAW on the square lattice with one end kept fixed and the other end subjected to a pulling force along (f_x) and perpendicular (f_y) to the preferred direction. At low temperature the conformation mimics a β sheet.

between the cases where the force is applied along the x or y directions, respectively, and we explain these observed differences using simple heuristic arguments. The PDSAW is a very restricted model and in order to further examine the role of anisotropy we introduce an anisotropic self-attracting self-avoiding walk (ASASAW) model and using exhaustive exact enumeration data for chains up to length $N=48$ study the combined effect of anisotropy and pulling in Sec. IV. The paper ends with a brief discussion in Sec. V.

II. PDSAW MODEL AND PHASE DIAGRAM

The PDSAW is a self-avoiding walk in which steps along some direction (say, the negative x direction) are forbidden. We study this model on a two dimensional square lattice. An attractive energy ϵ_u is associated with each nonbonded nearest neighbor [22]. At very low temperatures the attractive interactions dominate, and the PDSAW is in a collapsed phase, where the density of monomers in the bulk is close to one. The typical configurations of the chain mimics the β sheet [19] (see Fig. 1). At high temperatures thermal fluctuations are strong enough to break some of the interaction bonds and with increasing entropic contributions to the free energy the chain can be in an extended phase. A force $\vec{F}$ may be applied along some fixed direction giving rise to a stretching energy E_s arising from the applied force $\vec{F}$

$$E_s = -\vec{F} \cdot \vec{\alpha}, \qquad (1)$$

where $\vec{\alpha}$ is the end-to-end vector. In this paper we consider only the cases where the force is applied either along the x direction (f_x) or the y direction (f_y).

The phase boundary between the collapsed and the extended phase can be obtained by calculating the macroscopic shape of the collapsed phase at low temperatures. Let $\omega_x = \exp(f_x/T)$, $\omega_y = \exp(f_y/T)$, and $u = \exp(\epsilon_u/T)$, where T is the temperature. We set the Boltzmann constant k_B equal to 1. The energy of the configuration which mimics the β sheet is (see Fig. 1)

$$E = -\epsilon_u N + \frac{\epsilon_u}{2}(a_1 + a_2 + 2b) + \frac{\epsilon_u}{2}\sum_{j=0}^{b-2}|y_{j+2} - y_j|, \qquad (2)$$

where, as illustrated in Fig. 1, $a_1 = |y_1 - y_0|$ is the height (number of steps in the y direction) of the first column, $a_2 = |y_b - y_{b-1}|$ is the height of the last column, and b is the number of steps in the x direction.

Following the approach developed in Ref. [23], we express the sum appearing in Eq. (2) as a surface tension term. The macroscopic shape of the polymer is calculated and the value of ω_x at which the collapsed phase becomes unstable gives the critical value ω_x^c in terms of ω_y and u:

$$\omega_x^c = \frac{u}{(u-1)\sqrt{\omega_y}}[(\sqrt{u} - \sqrt{\omega_y})(\sqrt{u}\sqrt{\omega_y} - 1)]. \qquad (3)$$

Equation (3) gives the complete three-dimensional phase boundary. For $f_y = 0$ ($\omega_y = 1$), Eq. (3) reduces to the following simple expression for the critical force when pulling along the x direction:

$$\omega_x^c = \frac{u(\sqrt{u} - 1)}{\sqrt{u} + 1}. \qquad (4)$$

This coincides with the result obtained by transfer matrix methods [20]. However, that method is not easily generalized to the case where force is applied along the y direction. Equation (3), on the other hand, is sufficiently general to yield an expression for the critical force when pulling along the y direction. Setting $f_x = 0$ (or $\omega_x = 1$) yields the critical force when pulling along the y axis:

$$\omega_y^c = \left[\frac{1 + u^2 + \sqrt{1 + 2u^2 - 4u^3 + u^4}}{2u^{3/2}}\right]^2. \qquad (5)$$

For zero force (i.e., $\omega_x = \omega_y = 1$) the expression reduces to the exact value $u^c = 3.3829\cdots$ ($T = 0.8205\cdots$ if we set $\epsilon_u = 1$) at which thermal unfolding occurs. The exact phase boundaries obtained from Eqs. (4) and (5) are shown in Fig. 2 and compared to numerical results obtained for $N = 150$.

III. NUMERICAL ANALYSIS

Our numerical studies of the process of force induced protein unfolding are based on the exact enumeration of all possible conformations of the chain. This approach not only enables us to obtain precise estimates for the phase boundary, but also allows us to study the intermediate states crucial to events occurring during the mechanical stretching process [24–26]. In this study we have combined the power of parallel processing and transfer matrix calculations to extend the limit of earlier studies not just by one or two monomers but five times over. Thus we have extended from the previous longest chain length [21] $N=30$ to much longer chains of up to $N=150$ steps. The partition function is

$$Z_N = \sum_{N_p, \alpha_x, \alpha_y} C_N(N_p, \alpha_x, \alpha_y) u^{N_p} \omega_x^{\alpha_x} \omega_y^{\alpha_y}, \qquad (6)$$

where C_N is the total number of N-stepped PDSAWs having N_p nonbonded nearest neighbor pairs with end-to-end vector (α_x, α_y).
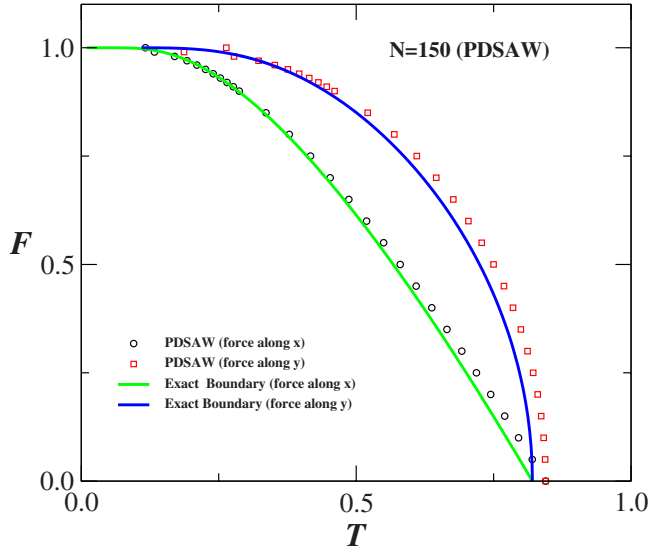
FIG. 2. (Color online) The globule-coil phase boundary in the force-temperature plane. The response to the force when applied along the y direction (squares) is distinctly different to the case where the force is applied along the x direction (circles). The continuous lines show the exact phase boundaries which are in excellent agreement with our numerical results for finite $N=150$.

The value of the transition temperature (for fixed force and finite N) can be obtained from the fluctuations in the number of nonbonded nearest-neighbor interactions. The fluctuations are defined as $\chi = \langle N_p^2 \rangle - \langle N_p \rangle^2$, with the kth moment given by

$$\langle N_p^k \rangle = \frac{\displaystyle\sum_{N_p, \alpha_x, \alpha_y} N_p^k C_N(N_p, \alpha_x, \alpha_y) u^{N_p} \omega_x^{\alpha_x} \omega_y^{\alpha_y}}{\displaystyle\sum_{N_p, \alpha_x, \alpha_y} C_N(N_p, \alpha_x, \alpha_y) u^{N_p} \omega_x^{\alpha_x} \omega_y^{\alpha_y}}. \tag{7}$$

When the fluctuations χ are plotted as a function of temperature the resulting graph (Fig. 3(a)) has a peak at the transition temperature. The inset shows that the height of the peak in the fluctuation curve grows as a power law with N, this being the hallmark of a phase transition. By setting $\epsilon_u = 1$ we obtain (for $N=150$) at zero force ($\omega_x = \omega_y = 1$) the transition temperature $T=0.8446$. This is already quite close to the value $T=0.8205$ obtained in the thermodynamic limit ($N \to \infty$). Figure 3(b) shows the variation in the transition temperature plotted against $1/N$ and we see a pronounced curvature for large N making an extrapolation to the limit $N \to \infty$ very difficult.

In Fig. 2 we show the force-temperature diagrams for $N=150$ when pulling along the x and y axis (circles and squares, respectively). These numerical estimates for the phase boundary are in excellent agreement with the analytical results (shown as solid lines) obtained from Eqs. (4) and (5). Thus exact enumeration technique works quite well even for small N as far as the phase diagram is concerned. This has also been seen earlier [27] in the case of the surface adsorption.
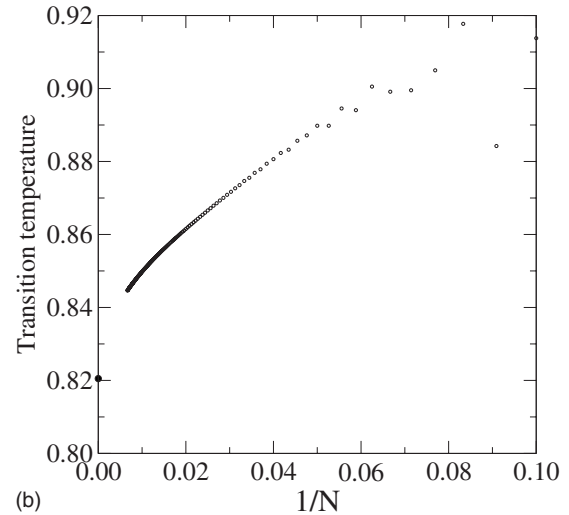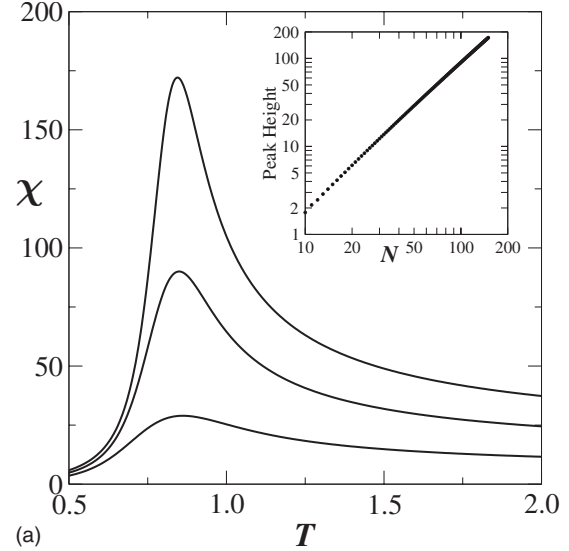

FIG. 3. (a) Fluctuations in the number of nearest-neighbor contacts (χ) as a function of temperature for different N. The inset shows how the peak height increases with N at the transition temperature. (b) The variation of the transition temperature as $N \to \infty$. The dot on the y axis marks the exact transition temperature.

Constant force and constant distance ensembles

Many biological reactions involve large conformational changes providing a well-defined mechanical reaction coordinate (e.g., the end-to-end distance of a biopolymer), which has been used in force spectroscopy experiments to follow the progress of the reaction [1,5]. Within the constant force ensemble (CFE) the theoretical predictions based on exact enumeration results provide a qualitative description of the outcomes of such experiments [21,28] (such as the existence of intermediate states and different pathways to unfolding). In Fig. 4 we have plotted the average extension as a function of the applied force. Figure 4(a) shows the result when the force is applied in the x direction and Fig. 4(b) when the force is applied in the y direction. In both cases we see the existence of several plateaus showing that there are many intermediate states between the collapsed and fully extended state. A major difference is that the number of these interme-
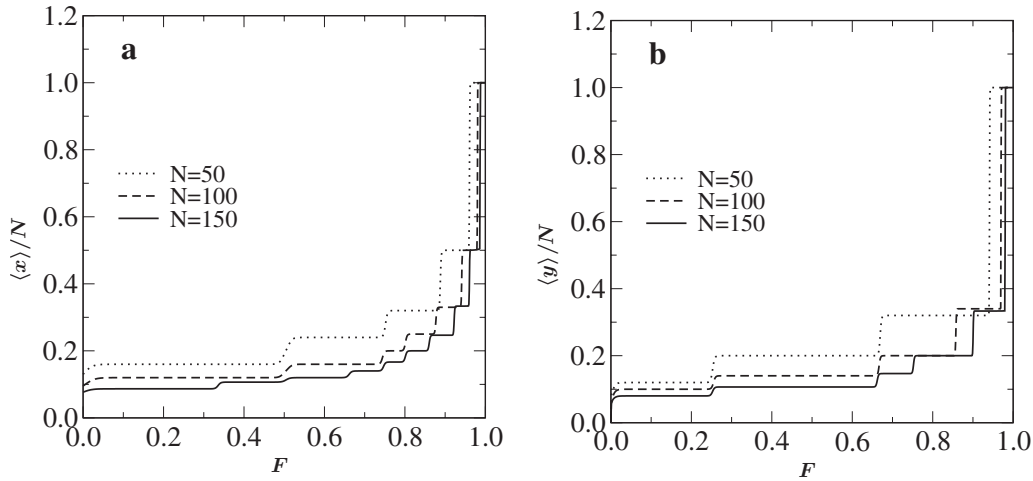
FIG. 4. Plots of the average extension $\langle x \rangle/N$ ($\langle y \rangle/N$) vs the applied force F for chain lengths $N=150$, 100, and 50 at fixed temperature $T=0.01$ with the force along the x direction (y direction).

diate states seems to grow much faster with the chain length N when pulling in the x direction as compared to pulling in the y direction.

The appearance of the plateaus in the force-extension curves as well as the differences between the two cases have a simple heuristic explanation. At very low temperature there are no entropic contributions to the free energy which is thus dominated by the energetic terms arising from nearest-neighbor interactions and the applied force. When pulling in the x direction we have to maximize the quantity $G=Fx+N_p$, where N_p is the number of contacts. For $F \rightarrow 0$ this means just maximizing m, and this is achieved by zigzag conformations inscribed in a rectangle which is as close to a square as possible so that $\langle x \rangle/N$ is close to $\sqrt{N}$. As the force is increased other configurations may become energetically favored, essentially corresponding to decreasing the width of the rectangle by a unit and increasing the length correspondingly (a more detailed explanation can be found in Ref. [29]; see also Ref. [30]). So the plateaus seen in Fig. 4(a) arise from inscribing a PDSAW of fixed length N in rectangles, going from right to left, of width $w=2,3,\ldots,\sqrt{N}$ as evidenced by the fact that these plateaus have height $\langle x \rangle/N=1/w=1/2,1/3,\ldots$. The types of conformations giving rise to the right-most plateaus are represented schematically in Figs. 5(a)–5(c). When pulling in the y direction we again get a competition between the force which tends to maximize the distance of the end point in the y direction and interactions which try to inscribe the PDSAW into a square. As illustrated in Figs. 5(d)–5(f) the conformations giving rise to the right-most plateaus are now those where the PDSAW is inscribed in a rectangle of length $l=3,5,7,\ldots,\sqrt{N}$. This can be seen in Fig. 4(b) where these plateaus have height $\langle y \rangle/N=1/l=1/3,1/5,\ldots$. Even lengths cannot occur because for these the end point would have a y component close to 0 giving only a small energetic contribution from the applied force. The upshot is that for a given length the number of plateaus when pulling in the x direction will be about twice the number of plateaus when pulling in the y direction.

Our longer series data also allows us to go a step further in analyzing the model in the constant distance ensemble

(CDE). This is the ensemble best suited to the analysis of experiments performed using apparatus such as atomic force microscopes. In Fig. 6 we have plotted the average force $\langle F \rangle$ [28] as a function of the extension when pulling in either the x or y direction. Striking differences between the two cases are obvious from these plots. Most obviously we note that at the low temperature $T=0.1$ the force extension curve obtained for pulling in the x direction shows an unzipping like transition characterized by having smooth plateaus. However, when the chain is being pulled in the y direction (at the same temperature), the force extension curve exhibits "saw-tooth-like" oscillations indicating that the transition is akin to shearing. This clearly demonstrates that even the nature of the unfolding transition can change dramatically solely by varying the pulling direction.

IV. ANISOTROPIC SELF-ATTRACTING–SELF-AVOIDING WALKS

The model described above has an exact solution and gives qualitative features similar to experiments. However,
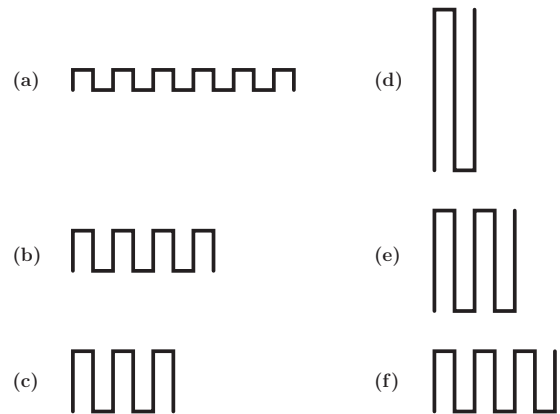

FIG. 5. Schematic diagrams of the configurations giving rise to the plateaus in the force-extension curves when pulling in the x direction (a)–(c) and along the y direction (d)–(f).
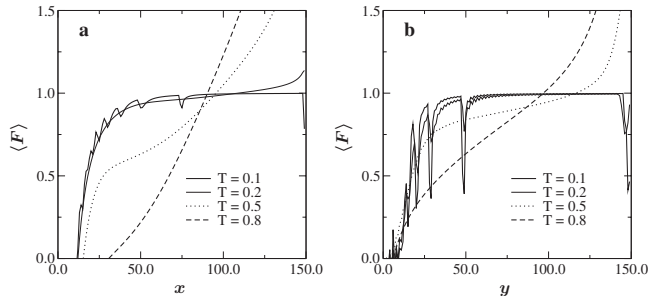
FIG. 6. Plot of the average force $\langle F \rangle$ vs the elongation at different temperatures T for chain length $N=150$. The marked difference due to a change in pulling direction is clear from these plots.

the physical constraints imposed by experimental setups has not been taken fully into account. For example, in experiments using atomic force microscopes, receptor and ligand molecules are attached to a substrate and a transducer, respectively, which introduce anisotropy in the systems. Also steric constraints due to the confinement imposed by the experimental setup can lead to a loss of entropy and thus result in modifications to the behavior of the chain. Furthermore the constraint of partially directing the walk so it cannot take steps in the negative x direction is not really appropriate to most experimental conditions. Such a constraint is typically only appropriate when the system is under flow or constant external field [31,32]. A more realistic model of polymers is provided by self-attracting–self-avoiding walks (SASAWs), which is well suited to the modeling of a linear chain in a poor solvent [18,22]. However, this model is isotropic in nature. In this paper we introduce anisotropy to the model. We achieve this by considering nearest-neighbor interactions with different strengths along the x and y directions as shown in Fig. 7(a). This is in accordance with real proteins where
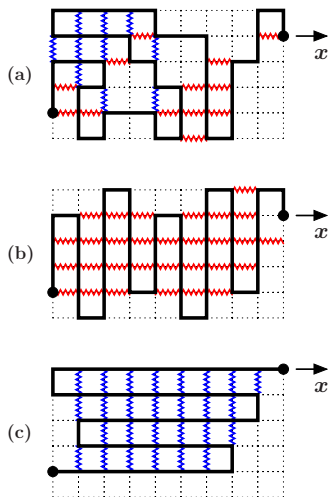

FIG. 7. (Color online) Schematic representation of ASASAWs on the square lattice. (a) Different nearest-neighbor interactions along the x and y directions introduce anisotropy in the model polymer. (b) Ground-state conformations which dominate the partition function similar to Fig. 1 when subjected to force along the x direction. (c) Same as (b) but resembles Fig. 1 when subjected to force along the y direction.
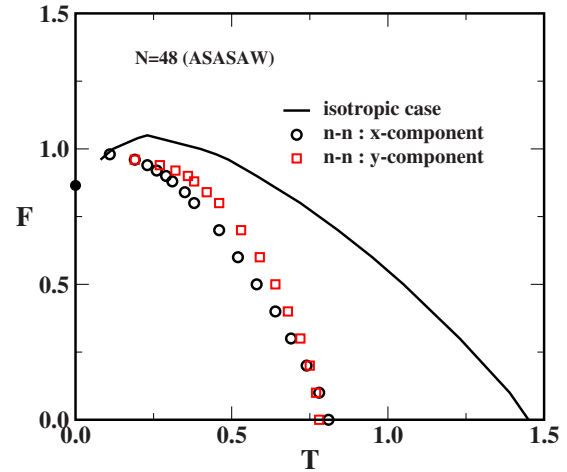

FIG. 8. (Color online) The force-temperature phase diagram for ASASAWs. The solid line represents the phase boundary for the isotropic SASAWs.

the interactions along different directions can differ by orders of magnitude [19]. Hence by changing the strength of the interactions one can vary the degree of anisotropy in the system and study the effect this has on the force-temperature phase diagram. The partition function for anisotropic self-attracting–self-avoiding walks (ASASAWs) may be written as

$$Z'_N = \sum_{(N_{px},N_{py},|\alpha|)} C_N(N_{px},N_{py},|\alpha|)u_x^{N_{px}}u_y^{N_{py}}\omega_\alpha^{|\alpha|}. \quad (8)$$

Here C_N is the total number of ASASAWs of N steps having N_{px} and N_{py} nearest-neighbor pairs along the x and y directions, respectively, while $u_x=\exp[-\beta\epsilon_x]$ ($u_y=\exp[-\beta\epsilon_y]$) are the Boltzmann weights associated with the nearest-neighbor interactions between nonbonded monomers along, respectively, the x and y directions.

The qualitative as well as quantitative features of the force-temperature phase diagram as shown in Fig. 8 for the isotropic case (i.e., $u_x=u_y=u$) remain the same as those reported in Ref. [28]. To make our model closely resemble the PDSAW discussed above, we set either $u_x=1$ or $u_y=1$ and apply a force along the x direction. For $u_y=1$ the ground state is dominated by configurations similar to the one shown in Fig. 7(b). This closely resembles the PDSAW model (Fig. 1) subjected to a force along the x axis and the nature of the transition is akin to an unzipping transition. On the other hand, for $u_x=1$ the ground state is dominated by configurations such as the one shown in Fig. 7(c). This closely resembles the configurations of Fig. 1 with a force along the y axis and consequently the nature of the transition is akin to a shearing-type transition. It should be noted that the number of ASASAWs C_N is different from the number of PDSAWs even if we put $u_y=1$. We observe a significant decrease in the transition temperature compared to SASAWs. This is caused by a decrease in entropy which allows the polymer to acquire conformations similar to a β sheet. The effect of surface confinement is also evident from these plots. The transition temperature is found to be less for $u_x=1$ in comparison to
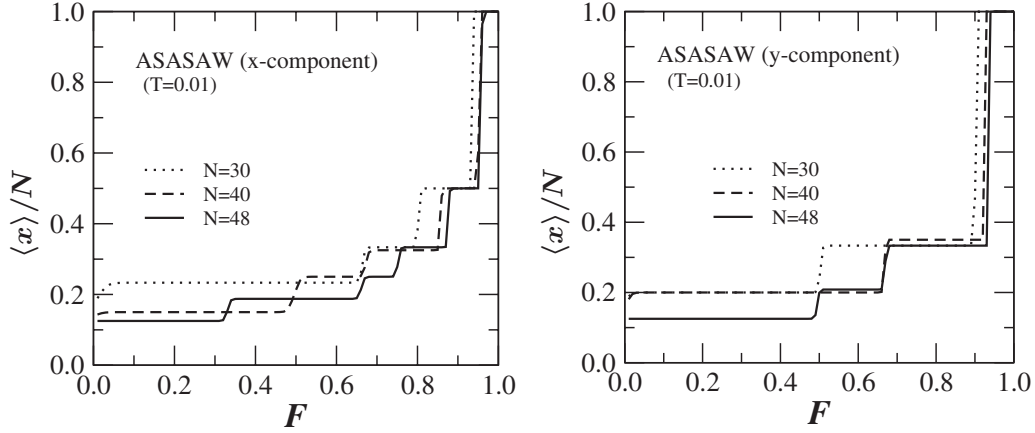
FIG. 9. Left panel: The average scaled elongation $\langle x \rangle / N$ as a function of the force with interactions along the x direction at fixed low temperature $T=0.01$ for different chain lengths. Right panel: Same as the left panel but for interactions along the y direction.

$u_y=1$. Another major difference between the ASASAW and SASAW phase diagrams is that there appears to be no reentrance in the ASASAW model when $u_x=1$ or $u_y=1$. It is well known that the reentrant behavior of the SASAW model is due to a nonzero ground-state entropy, that is, the number of configurations in the ground state grows exponentially with N (these configurations are just Hamiltonian walks inscribed in a rectangle with side lengths as close as possible to $\sqrt{N}$). For the ASASAWs we study here the ground states are, as argued above, folded sheets as in Figs. 7(b) and 7(c), respectively. The number of such configurations do not grow exponentially with N and are thus too few to give a nonzero ground-state entropy, which is why we do not see reentrance. However, if both u_x and u_y are greater than 1 then one may see a reentrant phase diagram.

The force extension curve shown in Fig. 9 not only shows the existence of intermediate states but also the emergence of new states depending on the direction of the interactions in accordance with the findings for PDSAWs. As the temperature is increased we observe in Fig. 10 (as expected) that the intermediate states are washed out due to the resulting increase in entropy. We also observe that the system attains a higher

stability against the force when the interactions are along the y direction and that intermediate states survive even at high temperatures as may be seen from Fig. 10.

Finally we analyze the ASASAW model in the constant distance ensemble. In Fig. 11 we have plotted the average force $\langle F \rangle$ [28] as a function of the extension when pulling in the x direction with interactions either along the x or y direction. The results are qualitatively very similar to those obtained for the PDSAW model (see Fig. 6). In particular, we note that the oscillation at low temperature are much more pronounced in the case where the interactions are in the y direction. As explained above (see Fig. 7) there is a close correspondence between the ground-state (low-temperature) configurations of the ASASAW with interactions in the x or y directions and the PDSAW with a force applied along the x or y direction, respectively. This close correspondence is reflected in the similarity of the results.

V. CONCLUSION

In summary we have demonstrated via the analytical solution for the phase boundary of PDSAWs as well as through high precision numerical calculations that changing the pull-
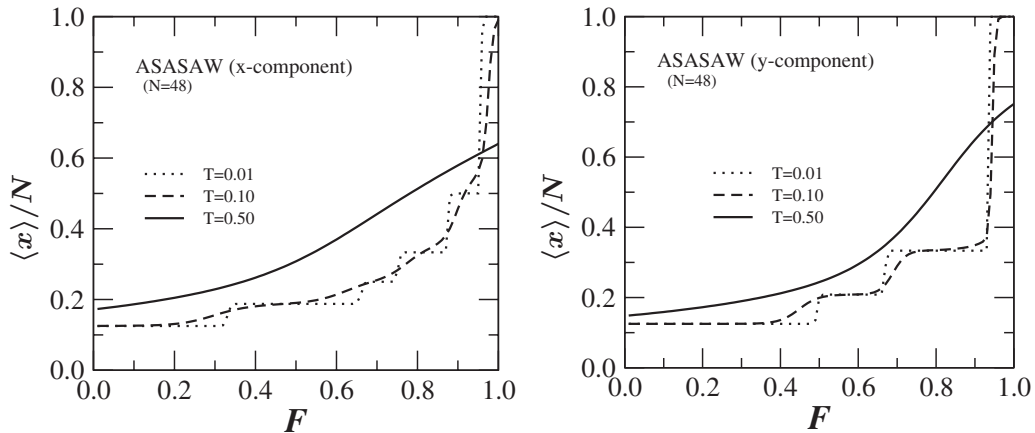

FIG. 10. Left panel: The average scaled extension $\langle x \rangle / N$ along the x direction as a function of the force at different temperatures with chain length $N=48$. Right panel: Same as the left panel but with interactions along the y direction.
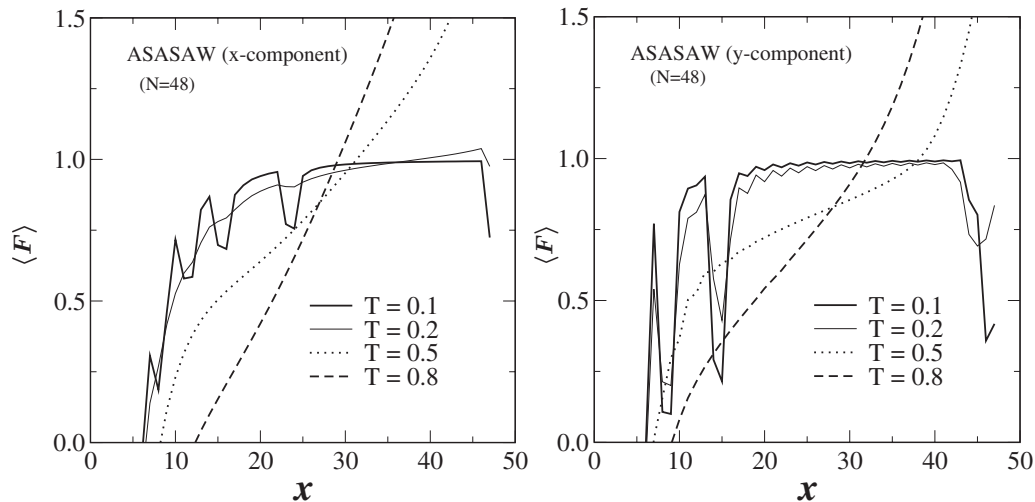
FIG. 11. Left panel: The average force $\langle F \rangle$ vs the extension x with interactions along the x direction alone at different temperatures with chain length $N=48$. Right panel: Same as the left panel but with interactions along the y direction.

ing direction can change the nature of the unfolding transitions and give rise to very different phase diagrams. The emergence of many new intermediate states suggests that there may be many pathways to the unfolding of a polymer. The findings for the PDSAW model have been confirmed by our study of ASASAWs. The inclusion of anisotropy in the traditional SASAW model of polymers gives unequivocal evidence that the features observed here for the PDSAW model are in fact generally true and not an artifact of the PDSAW model. In future additional work similar extensive Monte Carlo simulations and molecular dynamics studies are needed to better understand the role played by anisotropy

and how varying the pulling direction can help us gain a better and deeper understanding of biomolecules.

ACKNOWLEDGMENTS

[1] M. Rief *et al.*, Science **276**, 1109 (1997).
[2] M. S. Z. Kellermayer, S. B. Smith, H. L. Granzier, and C. Bustamante, Science **276**, 1112 (1997).
[3] L. Tskhovrebova, J. Trinick, J. A. Sleep, and R. M. Simmons, Nature (London) **387**, 308 (1997).
[4] C. Bustamante, Y. R. Chemla, N. R. Forde, and D. Izhaky, Annu. Rev. Biochem. **73**, 705 (2004).
[5] M. Carrion-Vazquez *et al.*, Proc. Natl. Acad. Sci. U.S.A. **96**, 3694 (1999).
[6] L. Serrano *et al.*, J. Mol. Biol. **224**, 783 (1992).
[7] A. E. Eriksson *et al.*, Science **255**, 178 (1992).
[8] D. J. Brockwell *et al.*, Nat. Struct. Biol. **10**, 731 (2003).
[9] M. Carrion-Vazquez *et al.*, Nat. Struct. Biol. **10**, 738 (2003).
[10] M. Kouza, C. K. Hu, and M. S. Li, J. Chem. Phys. **128**, 045103 (2008).
[11] A. Matouschek and C. Bustamante, Nat. Struct. Biol. **10**, 674 (2003).
[12] H. Dietz and M. Rief, Proc. Natl. Acad. Sci. U.S.A. **103**, 1244 (2006).
[13] H. Dietz, F. Berkemeier, M. Bertz, and M. Rief, Proc. Natl. Acad. Sci. U.S.A. **103**, 12724 (2006).
[14] M. Fixman, J. Chem. Phys. **58**, 1559 (1973).
[15] M. Doi and S. F. Edwards, *Theory of Polymer Dynamics* (Ox-

ford University Press, Oxford, 1988).
[16] J. F. Marko and E. D. Siggia, Macromolecules **28**, 8759 (1995).
[17] M. Rief, J. M. Fernandez, and H. E. Gaub, Phys. Rev. Lett. **81**, 4764 (1998).
[18] P. G. de Gennes, *Scaling Concepts in Polymer Physics* (Cornell University Press, Ithaca, 1979).
[19] T. E. Creighton, *Protein Folding* (W. H. Freemann, New York, 1992).
[20] A. Rosa, D. Marenduzzo, A. Maritan, and F. Seno, Phys. Rev. E **67**, 041802 (2003).
[21] S. Kumar and D. Giri, Phys. Rev. Lett. **98**, 048101 (2007).
[22] C. Vanderzande, *Lattice Models of Polymers* (Cambridge University Press, Cambridge, 1998);S. Kumar and Y. Singh, Phys. Rev. A **42**, 7151 (1990).
[23] The full details of the calculations will be given elsewhere.
[24] S. M. Altmann *et al.*, Structure (London) **10**, 1085 (2002).
[25] H. Dietz and M. Rief, Proc. Natl. Acad. Sci. U.S.A. **101**, 16192 (2004).
[26] I. Schwaiger *et al.*, Nat. Struct. Mol. Biol. **11**, 81 (2004).
[27] P. K. Mishra, S. Kumar, and Y. Singh, Physica A **323**, 453 (2003).
[28] S. Kumar, I. Jensen, J. L. Jacobsen, and A. J. Guttmann, Phys.

Rev. Lett. **98**, 128101 (2007).

[29] A. J. Guttmann, J. L. Jacobsen, I. Jensen, and S. Kumar, e-print arXiv:0711.3482.

[30] J. Krawczyk, A. L. Owczarek, T. Prellberg, and A. Rechnitzer, Europhys. Lett. **70**, 726 (2005).

[31] A. S. Lemak, J. R. Lepock, and J. Z. Y. Chen, Phys. Rev. E **67**, 031910 (2003).

[32] A. S. Lemak, J. R. Lepock, and J. Z. Y. Chen, Proteins: Struct., Funct., Genet. **51**, 224 (2003).